PHYSICAL REVIEW A VOLUME 15, NUMBER 1 JANUARY 1977

Charge exchange between multicharged ions of C, N, and O and molecular hydrogen*

D. H. Crandall, M. L. Mallory, and D. C. Kocher
Oak Ridge National Laboratory, Oak Ridge, Tennessee 37830
(Received 20 July 1976)

Cross sections for single- and double-electron capture have been measured for incident ions of C, N, and O with initial charges $+3$ to $+6$ colliding with molecular hydrogen at velocities between 0.3×10^8 and 1.2×10^8 cm/sec. The single-electron-capture cross sections for a particular incident charge are nearly constant with changing velocity. The single-capture cross sections range from about 7×10^{-16} cm^2 for $+3$ incident ions to 40×10^{-16} cm^2 for $+6$ incident ions. Double-electron-capture cross sections are roughly one order of magnitude smaller. The data are qualitatively interpreted on the basis of the molecular potential-curve model for slow collisions.

I. INTRODUCTION

For collisions of ions and atoms at velocities near and less than the velocities of the electrons in the atoms, the exchange of electrons is generally the largest inelastic process. Such charge exchange not only tests understanding of atomic collisions, but is also an important process in many physical phenomena. Electron transfer has been extensively investigated, but collisions of multicharged ions with atoms or molecules at velocities below the Bohr orbit velocity have received little attention, partly because of the difficulty of producing beams of slow multicharged ions.

Recently, specific interest in electron transfer involving multicharged ions has been stimulated by the need for data in several areas. In the high-temperature plasmas encountered in astrophysics and controlled thermonuclear research, heavy ions (often thought of as impurities) exist in fairly high charge states. Electron-transfer cross sections are large for velocities corresponding to the temperature of these plasmas. Thus, even though plasmas are dominated by electron collisions, charge transfer may modify plasma properties and influence emissions of light or particles which are observed in plasma diagnostics. There are other specific related problems apart from plasma modeling and diagnostics. For example, in astrophysics the degree of ionization of ions in the cool, low-density interstellar medium may be controlled by charge transfer.[1] In fusion research, the heating of a thermonuclear plasma by neutral beam injection may be impaired by charge transfer between the injected beam and multicharged impurity ions at the outer edges of the plasma.[2] Since electron transfer to multicharged ions from neutral gases is expected to occur predominantly into excited states, charge exchange is a possible mechanism for producing a population of excited states with enough energy for ultraviolet or x-ray lasers.[3,4] This partial list of problems requiring data on electron transfer with multicharged ions provides strong motivation for research in this area.

Charge exchange involving multicharged ions is of fundamental interest as well. The theories of electron transfer divide into slow and fast velocity regimes determined by whether the collision time is long or short compared to electron orbit times. For the slow collisions of present interest, successful calculations of electron-transfer cross sections have been based on viewing the collision event as the formation of a quasimolecule and modeling the response of the electrons to the changing potentials as the nuclei approach and recede during the collision. With multicharged ions, dominance of features such as formation of excited states and multiple electron transfer provide new challenges for the comparison of theory and experiment.

This paper presents data for various ions of C, N, and O incident on molecular hydrogen at velocities between 0.3×10^8 and 1.2×10^8 cm/sec for reactions

$$X^{+i}+H_2 \rightarrow X^{+f}+(H_2 \text{ products})^{+(f-i)} . \quad (1)$$

Collision systems with fewest electrons are most amenable to quantitative physical understanding. In addition, hydrogen (or deuterium) is the principal constituent in both astrophysical and thermonuclear plasmas while C, N, and O are significant multicharged impurities in these plasmas. Thus both theory and application single out atomic hydrogen as the most interesting target, with molecular hydrogen, protons, and helium also of considerable interest. The present results partially fulfill the need for accurate data. The cross sections obtained in this experiment are interpreted in light of the quasimolecule model and are com-

pared with recent theoretical calculations and other related experiments.

II. EXPERIMENTAL TECHNIQUE

A. Ion source

The primary obstacle to experiments with multicharged ions at low velocities has been the difficulty of producing slow ion beams. The ion source for the present experiments relies on magnetic confinement of an intense discharge and is referred to as a cold-cathode Penning ion gauge (PIG) type. The present ion source was developed for use in the Oak Ridge Isochronous Cyclotron and has been described in detail elsewhere.[5,6] The source is operated in a continuous (dc) mode and is capable of producing a large variety of partially stripped ions of charge up to 9 or 10.

In the configuration employed for the present experiments (see Fig. 1), ions are extracted transverse to the magnetic field so that ion cyclotron orbital motion results. The ions are extracted into a region where curved electrostatic plates provide a crossed electric field. With all other parameters held constant, the electrostatic field can be varied so that only ions with a particular mass-to-charge ratio are passed through the exit slit at the edge of the magnetic field. The selected ion beam is then transported to the collision chamber. The configuration of ion source and magnetic-electrostatic fields imposes practical limitations on the range of energies at which ion beams can be accelerated. At low extraction potentials, the ion trajections do not enter the region of the electrostatic field. At high extraction potentials, the electrostatic deflection potential exceeds voltage holding capability. The practical range of ion beam energies varies somewhat with charge and mass but is roughly 5 to 30 kV times the charge of the ion for C, N, and O ions. The precise value of electrostatic field required to extract a particular ion depends on other parameters

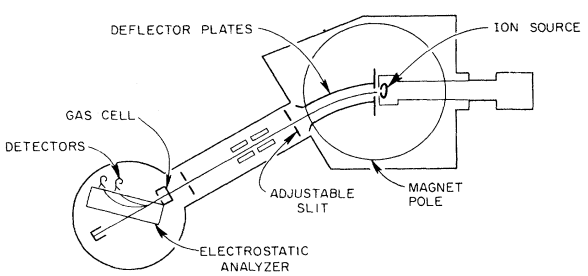

FIG. 1. Schematic of the apparatus discussed in Sec. II A and C.

such as magnetic field, source position, extraction angle, etc. Thus, unambiguous identification of the ion beam is aided by the charge state analysis which is an indigenous part of the present collision experiments.

B. Cross-section determination

A schematic diagram of the experiment is shown in Fig. 1. Incident ions undergo charge-changing collisions within the gas cell, and the subsequent charge-state analysis allows determination of charge-transfer cross sections. For single-collision conditions and detection of all ions in each of the final charge states, cross sections are obtained from the relationship

$$N_f = N_i \sigma_{if} nl, \tag{2}$$

where N_f is the number of ions in a given final charge state (in this case formed by charge exchange), N_i is the number of primary incident ions of charge $+i$, n is the density of molecules in the gas cell, l is the length of the gas cell, and σ_{if} is the cross section to be measured.

In applying Eq. (2), a number of precautions must be observed. All of the incident particles must be accounted for, and the probability of any particle suffering more than one collision should be negligible. All of the incident ions should be of a particular atomic species, charge, and electronic state. All collisions should take place within the gas cell, and n and l need to be precisely measured quantities. The uncertainties in realizing these conditions are evaluated in the following four sections.

C. Geometry

The collision geometry determines whether or not some of the above conditions are adequately satisfied. The ion beam was highly collimated at the gas cell so that only a small fraction of the original beam participated in the collision experiment. A 1-mm-diam collimator was placed 13 cm before the gas cell, and the gas cell entrance was a 0.25-mm aperture. The gas cell was 1.23 cm in length, and the exit aperture was 1.0 mm in diameter. The entrance of the parallel-plate electrostatic analyzer[7] was located 2.0 cm after the gas cell. The analyzer was fitted with large apertures, entrance 0.3 cm wide by 1.0 cm high and exits appearing to be 1.0 cm circular, when viewed at the 45° beam exit angle. The exits were variously spaced from 13 to 21 cm along the front plate from the entrance with channel electron multipliers[8] mounted as detectors.

The collision geometry provided a number of advantages. First, the ion beam intensity was

sufficiently diminished by the collimation that individual incident ions could be counted by a channeltron. Second, the geometry allowed full transmission of incident and scattered beam particles through the analyzer. Specifically, for accurate alignment of the system, any ion entering the gas cell and scattered vertically by less than about 2° would be detected, whereas, in the horizontal plane, because of the beneficial effect of analyzer focusing, particles scattered up to about 4° would be detected. Third, the small entrance and exit apertures of the gas cell allowed high differential pressures between the gas cell and collision chamber (about 5×10^{-7} Torr in collision chamber for 1×10^{-3} Torr in the gas cell). The effective lengthening of the gas cell by effusion of gas through end apertures was minimized by the small openings. The short gas cell allowed relatively high pressures without introducing a significant multiple-collision probability.

D. Determination of physical quantities

The single-electron transfer cross sections were obtained by simultaneously counting the number N_i of incident ions of X^{+i} and the number N_f of scattered ions of $X^{+(i-1)}$. The procedure is illustrated in Fig. 2, which shows the count rate at each detector as a function of analyzer voltage for a particular case. For a given detector, peaks in count rate at various analyzer voltages correspond to the different charge states of ions which have the incident velocity. For a stable incident ion beam and for single-collision conditions, the cross sections for charge transfer of one or more electrons could be obtained from the heights of each of the charge state peaks of either detector. However, to avoid relying on ion beam stability, and to readily subtract background, both detectors were used. The spacing of detectors was set according to the ratio of charges of the incident and desired charge-changed ions. The analyzer voltage was set to a value where the primary incident ion was detected in one detector (i channel) and the charge-exchanged ions were incident in the other detector (f channel). For the case shown in Fig. 2, this voltage is indicated by an arrow. The number of counts in each detector were then accumulated until a preset number of incident ions were counted. This procedure was repeated with and without target gas in the gas cell; background counts in the exchange channel with no gas in the collision cell were subtracted from the scattered particle signal. Typically, 10^5 primary incident ions were counted at a rate near 10 kHz. For single electron charge transfer, the background was usually 1% due primarily to charge exchange along the total flight path of the ion beam. Gas was added to the collision cell until an additional 1–2% of the incident ions underwent single-electron transfer.

This technique relies on both detectors having the same counting efficiencies. For most of the data, the channeltrons were operated with the input at ground potential and no grid or other obstruction to the beam. The counting efficiency for these reasonably fast ions is expected to be 100%.[9-11] The relative counting efficiency of the two detectors was checked by deflecting the primary beam onto either channeltron. Within beam stability limits (about ± 5%), the count rate was always the same. This check was repeated after any "retuning" of the ion beam.

For these experiments, single charge transfer

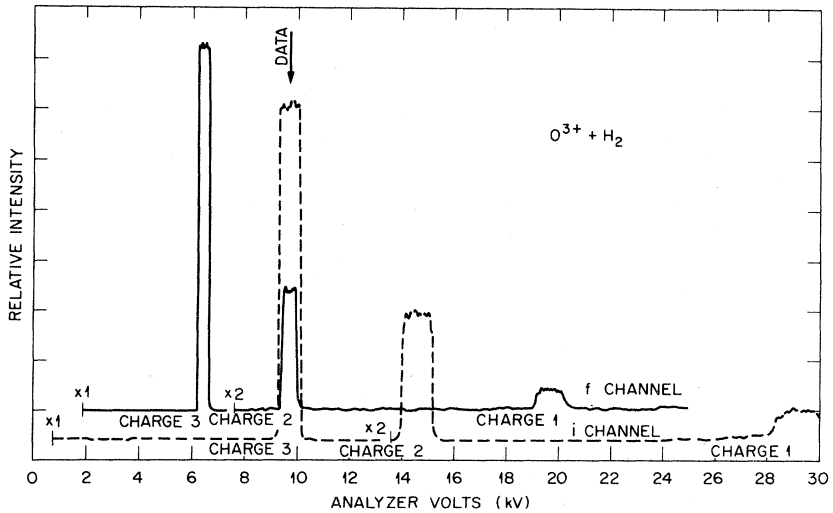

FIG. 2. Count rate into each detector as a function of analyzer voltage for $O^{3+} + H_2$ at 10 kV with gas cell pressure much higher than used in the experiment. Dotted line is detector for incident beam (i); solid line is detector for charge-exchanged beam (f). Arrow indicates voltage setting for data collection for single-electron transfer.

should be the only significant source for loss of particles from the incident beam. Double electron capture was found to be about an order of magnitude smaller. From close examination of graphs like Fig. 2, ionization to higher charge states is at least two orders of magnitude less than single electron pickup for all present cases so that ionization cannot account for a significant loss of incident beam particles. Angle or energy scattering out of the acceptance geometry is negligible for this experiment. A correction was made for the particles lost from the primary beam to single-electron capture by adding the increase of particles in the charge-exchanged beam, N_{i-1}, to the total incident or primary beam particle count N_i. This correction was generally about 2% and an uncertainty of ± 2% is allowed for the overall determination of the number of incident ions.

A further check for single-collision conditions was obtained by observing the linearity of increase in the number of exchanged particles N_{i-1}, with increasing gas cell pressure; or, alternatively, checking that the cross section as calculated from (2) was constant with increasing gas pressure. These checks indicated that single-collision conditions persist to about a factor of 4 greater pressures than used in the experiments and support the conclusion that the only significant loss of particles out of the primary beam is to single charge transfer.

Less stringent conditions were allowed for the double-electron-transfer cross-section measurements. The ratio of double transfer to single transfer was obtained directly from comparisons of peak heights on data plots like Fig. 2 with low gas pressure in the cell and with background subtracted. This technique relies on ion beam stability over a period of about 2 min during which 5–10% intensity variation was not uncommon, which resulted in degraded reproducibility for the double-electron-transfer cross sections. In addition, for the double-transfer determinations, higher pressures were used resulting in as much as 7 or 8% of the primary ions undergoing single transfer. The correction for incident ions lost to single-electron pickup was applied as described above. The uncertainty in N_i and the accompanying possible error due to multiple collisions are estimated to be ± 7% for the double-transfer measurements.

E. Pressure measurement

Gas was admitted to the collision chamber through a flexible coupling about 1.3-cm diameter by 22-cm length. The flexible coupling allowed rotation of the gas cell and analyzer out of the ion beam so that the full beam could be passed through the vacuum chamber to other experiments. The pressure was measured by the capacitance manometer at the entrance to the flexible coupling. The pressure in the gas cell differs from that at the manometer because of the conductance of the flexible coupling relative to that out the ends of the gas cell. This correction was measured directly as illustrated in Fig. 3. The 0.25-mm aperture was assumed to have negligible conductance compared to the 1.0-mm aperture and was removed so that a McLeod gauge could be coupled directly into the gas cell. The gas cell was mounted in a large vacuum vessel with the same couplings and pressure measurement system as during the collision experiments. Comparisons were made over the entire experiment pressure range with the McLeod gauge cooled[12,13] to about 0 °C and at room temperature with H_2 and He working gas. Figure 4 shows the comparison of the McLeod gauge and capacitance manometer pressure readings. The measured ratio is constant over the pressure range with an average value of 0.85. The ratio was estimated using calculated conductances to be 0.90 in reasonable agreement with the measured value. For cross-section determination, the capacitance manometer values were multiplied by 0.85. The capacitance manometer was compared directly with the McLeod gauge and another capacitance manometer by coupling all three devices directly to the large volume at static pressure. The direct comparison showed agreement among the three devices to better than 2%.

The physical length of the gas cell was accurately measured by a micrometer, and the effective addition to this length by effusion out of the end holes was estimated to be one half the diameter of

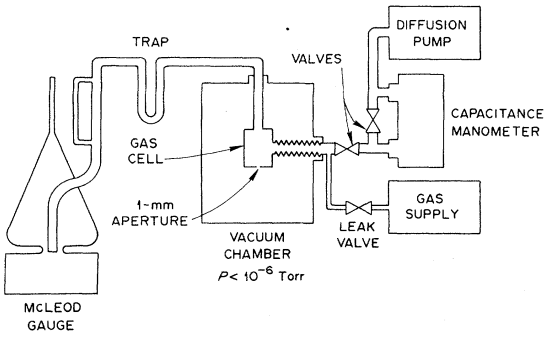

FIG. 3. Arrangement for direct measurement of actual gas cell pressure by McLeod gauge, relative to pressure measured at gas input point by capacitance manometer. Gas supply, capacitance manometer, and gas cell are as used for charge-exchange data except that 0.25-mm-input aperture of gas cell is replaced by McLeod gauge access.

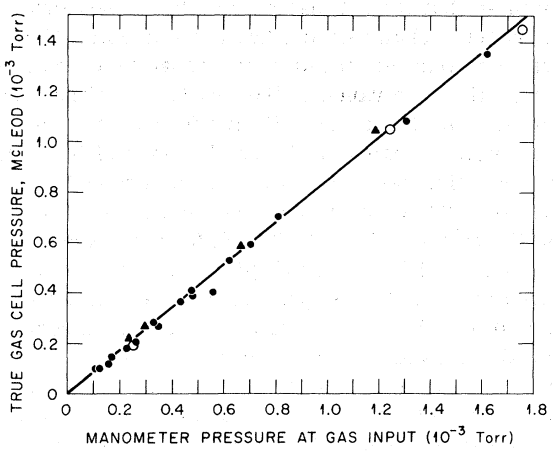

FIG. 4. Actual pressure in gas cell vs pressure measured at manometer. Solid points—hydrogen gas with McLeod gauge at −5 °C; open circles—hydrogen gas with McLeod gauge at +25 °C; triangles—helium gas with McLeod gauge at 0 °C.

each hole. Most data were acquired with a gas cell 1.23 cm long with 0.25-mm entrance and 1.0-mm exit aperture, giving an effective length of 1.30 cm. Some data were taken with a longer cell (2.54 cm) and three different diameter entrance holes (1.0, 0.5, 0.25 mm). Data with the different gas cells and apertures all agreed to within about 10% after conductance and effusion corrections were applied.

With no gas input to the cell the pressure in the cell is expected to be near the base pressure of the vacuum system (2×10^{-7} Torr). The only monitor on the evacuated cell pressure was the capacitance manometer which could detect no pressure difference between the gas cell and the separate reference vacuum of the manometer (configuration as in Fig. 3.). Since the reference pressure was about 2×10^{-6} Torr, and the lowest pressure difference detectable by the manometer is a few $\times10^{-6}$ Torr, the evacuated cell pressure is asserted to be at least as low as 5×10^{-6} Torr. With 1×10^{-3} Torr pressure in the gas cell, the vacuum-chamber pressure rose to about 5×10^{-7} Torr. A test for the effect of this pressure rise on background was carried out by partially closing the valve to the chamber pump so that a similar rise occurred without gas added to the cell. The increase in charge-transfer background due to the rise in vacuum chamber pressure was negligible up to chamber pressure above 2×10^{-6} Torr.

High-purity gases were used, but some uncertainty should nevertheless be allowed in the cross sections for gas contamination. The gas feed system, of vacuum-tight copper tubing, was evacuated frequently to pressures of a few mtorr and the closed system held pressure below 50 mTorr for over 8 hours. During use, the tubing was filled to regulated pressure of about 20 lbs. Given these vacuum conditions and careful procedures with gas handling, it is reasonable that the target gas in the collision cell was pure to parts in 10^4 or better. To estimate the uncertainty in cross sections due to gas impurity, we allow for contamination of parts in 10^3 and allow for a difference in cross section between H_2 and impurity of a factor of 10 to 50. This estimate gives a high confidence limit on the effect of impurities on measured cross section of 5%.

F. Uncertainties

Table I presents estimated uncertainties from various sources. The average reproducibility is given at 90% confidence level for a few data points which were repeated on separate experimenting days, and in some cases with different length gas cells and different apertures. These reproducibilities are taken as representative for all data points. Other uncertainties are estimated at a high confidence level and the independent uncertainties are combined in quadrature. The resultant total absolute uncertainties of ±15% for single-transfer cross sections and ±22% for double capture do not include any allowance for the possibility of excited states in the incident beam which will be discussed in Sec. III E.

III. RESULTS AND DISCUSSION

A. Single-transfer cross sections

The cross sections for single-electron capture for various ions of C, N, and O incident on H_2 are shown in Figs. 5, 6, and 7, respectively. All of the single-transfer cross sections are nearly independent of velocity. However, for all cases the cross sections σ_{43} are large and increase with decreasing velocity to the extent that they violate

TABLE I. Summary of uncertainties.

Source	Single transfer (%)	Double transfer (%)
Reproducibility (90% CL)	±6	±15
Pressure + conductance	±10	±10
Temperature (±8 °C)	±3	±3
Effective length of gas cell	±5	±5
Gas purity (maximum effect on cross section)	±5	±5
Incident beam (N_q)	±2	±7
Relative counting efficiency	±5	±5
Quadrature sum	±15%	±22%

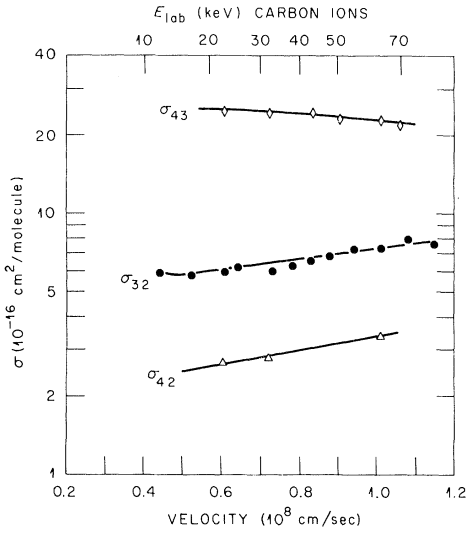

FIG. 5. Electron-capture cross sections σ_{if} for carbon ions incident on molecular hydrogen. The initial charge is i and final charge is f.

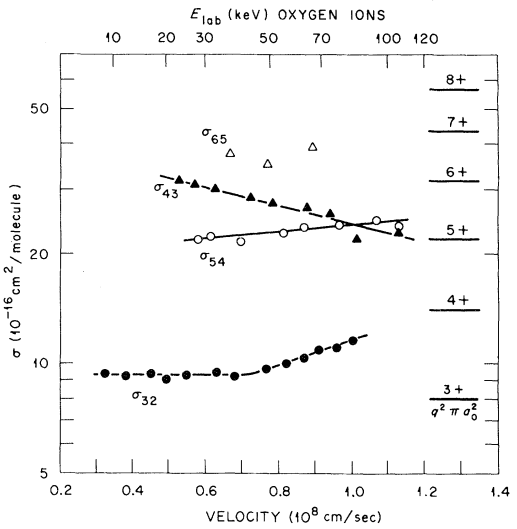

FIG. 7. Single-electron-capture cross sections σ_{if} for oxygen ions incident on molecular hydrogen.

the pattern that single transfer increases with increasing incident charge. These general features can be interpreted by employing a few qualitative aspects of the quasimolecular model for slow collisions.

The initial state of a multicharged ion plus a neutral molecule has potential energy that is relatively constant as a function of internuclear separation for distances greater than the size of the atom. For any final state consisting of two ions

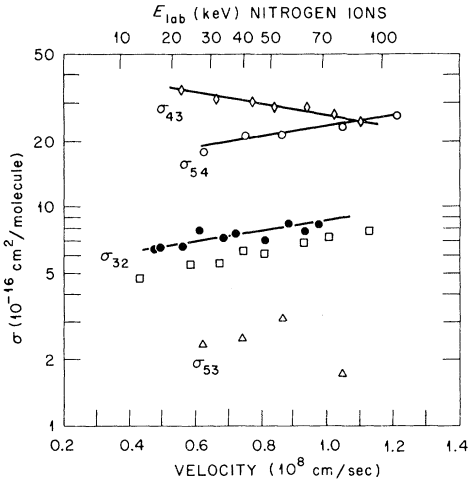

FIG. 6. Electron-capture cross sections σ_{if} for nitrogen ions incident on molecular hydrogen. Open squares are data for σ_{32} from Ref. 32; all other points are present data.

(which have a long-range Coulomb repulsion) the potential energy increases with decreasing internuclear separation beginning at large nuclear separation. Those two-ion final states which have separated energies of 5–50 eV lower than the initial state can have potential curves that intersect that of the initial state at internuclear separations about a_0 (the Bohr radius) and larger. Initial and final states having potential curves that cross at large internuclear separation (many a_0) do not interact. Thus for the present case of multicharged ions plus neutral target proceeding to final states of two ions, those final states that have separated atom energies very close to the initial state will have curve crossings at such large internuclear separation that electron transfer is not favored. Those initial and final states having curve crossings at separations of a few a_0 will interact such that potential-curve crossings are avoided. In this region the probability of transit of the colliding system to the final state is sensitive to the precise potential energies, the strength of interaction of the nearby energy levels, and the velocity of the collision.

For the cross sections studied here, it is likely that several product states are populated which have avoided curve crossings with the initial state at separations of the order of a few a_0. Curve crossings at these moderately large internuclear separations result in the large cross sections observed and the availability of several such interactions with different product states could produce the observed constancy of the total cross sections with changing velocity.

The interaction of initial and final states decreases with increasing electronic excitation of the final states. Thus, charge transfer into excited states decreases with increasing principal quantum number n of the final ion state. This additional qualification helps in interpreting the anomalously large cross sections, σ_{43}. Because of the final-states Coulomb repulsion, electron transfer will be largest into final states of the system having 10–30 eV energy defect relative to the initial state; however, for more highly charged incident ions colliding with a neutral target, the final states meeting this criterion have higher electronic excitation. Examination of atomic energy levels[14] reveals that for 4^+ to 3^+ transfer with C, N, or O ions there are numerous final states with $n \leq 3$ which satisfy the energy defect criterion, but for 5^+ to 4^+, the satisfactory levels have $n \geq 4$. While the cross sections generally rise with increasing incident charge, it is not unreasonable that σ_{43} can be larger than σ_{54} because of the effect of electronic excitation of final states on the total electron transfer. For higher incident charge the relative effect due to high electronic excitation in the final states becomes less dramatic so that cross sections again increase with increasing incident charge.

For the present case, vibrationally excited levels of H_2^+ and dissociated $H^+ + H$ states of the target are also possible product states. This relatively broad range of final excited target states can absorb some of the energy which would otherwise result in excitation of the final multicharged ions. The multicharged ions are still likely to be formed in excited states, but the number of such levels which can contribute to the total transfer cross section may be larger in the present case than with neutral-atom targets. Some information on this question exists from measurements we have made with the same ions but with helium target. For $O^{3+} + He \rightarrow O^{2+} + He^+$ the cross section is one third that for molecular-hydrogen target at all velocities, and for $N^{5+} + He \rightarrow N^{4+} + He^+$ the cross section is one half that for molecular-hydrogen target at all velocities. Thus there is no observed difference in the cross sections that can be identified as characteristic of a molecular target. It has been pointed out by Olson and Salop[23] that the cross section for molecular H_2 is expected to be lower than for H^0 target at these low velocities where potential-curve crossings dominate the cross section. This reduction in charge transfer for the molecular case is primarily due to the Franck-Condon factors for overlap of various vibrational levels which reduce the matrix elements connecting initial and final states of the system.

B. Direct comparisons to theory

A few charge-transfer calculations with multicharged ions for collision velocities $v \lesssim 1 \times 10^8$ cm/sec have been attempted. The simplest system to consider is a one-electron diatomic molecule. Electron transfer for such systems as $X + X^+ \rightarrow X^+ + X$ have been successfully predicted with a quasimolecule model.[15,16] A general approach for estimating the transition of the electron between potential curves of the colliding system, developed by Landau[17] and Zener,[18] has been widely applied, even with multicharged ions.[19] This method is most reliable when the significant potential-curve crossings are well defined at reasonably large internuclear separation, and has been applied by Salop and Olson[20] to electron transfer in collisions of fully stripped C, N, O, Ne, Si, and Ar with atomic hydrogen. At collision velocity of 0.1×10^8 cm/sec, the predicted cross sections are spread over two orders of magnitude, 1 to 100×10^{-16} cm^2, with individual cases being sensitive to exact nature of the curve crossings. At $v = 0.8 \times 10^8$ cm/sec, the calculated cross sections are reasonably constant with increasing velocity and scale as $q^{3/2}$. The present data are qualitatively similar to predictions of Refs. 19 and 20, but precise cross-section prediction for individual cases relies on accurate calculation of coupling and potential curves for the particular case considered. For $C^{4+} + He$ and $B^{3+} + He$, accurate potential curves have been combined with close-coupling calculation of the electron transfer between curves over a wide range of internuclear separations, and quantitatively correct cross sections were predicted.[21,22] Such calculations on collisions of near fully stripped ions with H and accurate measurements of the same systems should definitively test the reliability of these techniques.

In many cases, the number of interacting potential curves makes such detailed numerical calculation prohibitive. Olson and Salop[23] have attempted to develop a method for applying the one-electron diatomic molecule model with Landau-Zener curve crossing to such cases. A large number of one-electron coupling matrix elements are computed and parametrized by the initial charge q and internuclear separation. By empirically deducing a functional form for the matrix elements, cross sections can be calculated using an extension of the Landau-Zener method. The calculation has been applied for H, H_2, and rare-gas targets. The comparison with present data for incident ions of charge 4, 5, and 6 at collision velocity 0.7×10^8 cm/sec shows agreement better than $\pm 30\%$ except for σ_{54} for N^{5+} and O^{5+}, where present data are about $\frac{2}{3}$ of the calculation. Com-

parison of Olson and Salop calculations with data of Müller, Klinger, and Salzborn[24,25] for Ar^{+i} in Ar also shows reasonable agreement.

C. Double-transfer cross sections

Figures 5, 6, and 8 show that double-electron transfer is roughly one order of magnitude smaller than single transfer. For oxygen ions (Fig. 8) double transfer is even smaller, but σ_{64} rises so rapidly that it might become significant relative to σ_{65} at velocities lower than those studied. This rapid rise of σ_{64} with decreasing energy is qualitatively similar to the $C^{4+}+He$ case[21] and may be due to a single potential-curve crossing at fairly large internuclear separation, favoring double transfer. Double-electron transfer is usually significantly lower than single transfer (see Refs. 19, 24, 26–28), but in particular cases, double transfer can dominate over single transfer.[21,29]

D. Comparison–higher energy and scaling

At collision velocities above 4×10^8 cm/sec considerable data exist[28] and qualitatively successful calculations trace back to the classical model of Bohr[30] and quantum model of Brinkman and Kramers.[31] Based on these results, it is anticipated that the present cross sections, if extended to higher energy, would begin to decrease rapidly at some velocity between 2 and 6×10^8 cm/sec. Also based on the many high-energy results some scaling laws have been fairly successful. A widely used scaling rule is that the charge-changing cross sections be proportional to q^2. For electron capture this rule is appropriate only in the high-velocity regime for cases where the electron binding energy in the unfilled shell of the incoming ion is larger than $\frac{1}{2}mv^2$ where m is electron mass and v is the collision velocity.[27] The present data should tend to this limit at velocities above those measured. For comparison, the quantity $(\pi a_0^2)q^2$ is plotted on Fig. 7. While the data do not fit this scaling, they are of this magnitude and indicate some tendency toward such scaling at the highest velocity.

E. Comparison with other data

Data from Flaks and Ogurtsov[32] for σ_{32} of N^{3+} in H_2 are shown on Fig. 6 with the present data. Their data are about 10% lower than present values—within the uncertainties of either experiment. They used significantly different geometry (longer gas cell and lower pressure) and different detectors; the agreement is highly satisfactory.

Data for Ar^{4+} and Ar^{5+} were obtained in order to compare to data of Klinger, Müller, and Salzborn[24,25] (Fig. 9). The data of Klinger *et al.* have been reduced 20%[33] from values given in Ref. 24 to reflect a more accurate determination of their effective scattering length. However, their data remain consistently 40% greater than our measurements, a discrepancy equal to the sum of uncertainties of the separate measurements. The ratios of cross sections for increasing numbers of electrons transferred in one collision are well reproduced. The present data for Ar^{5+} were contaminated slightly by the presence of O^{2+} in the incident beam which was revealed by examination

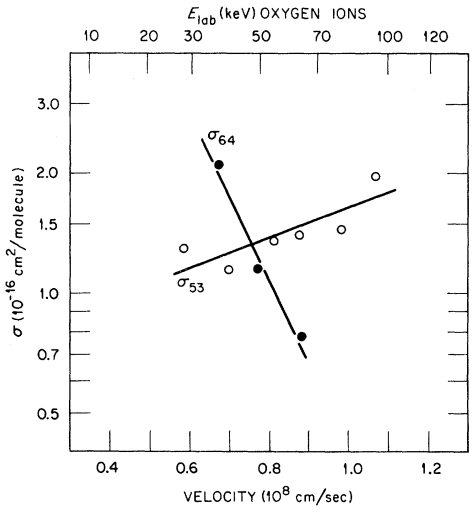

FIG. 8. Two-electron capture cross sections σ_{if} for oxygen ions incident on molecular hydrogen.

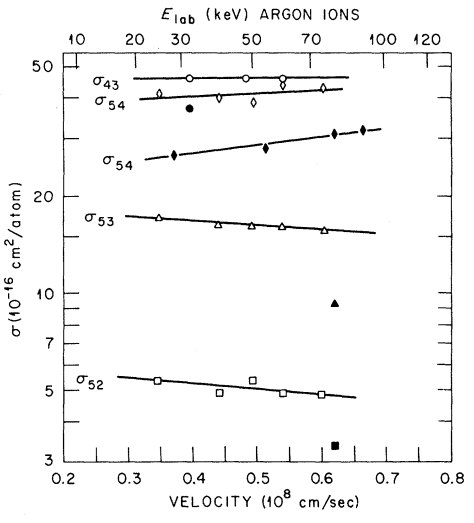

FIG. 9. Electron-capture cross sections for argon ions incident on argon. Present data: ●, σ_{43}; ◆, σ_{54}; ▲, σ_{53}; ■, σ_{52}. Data of Refs. 24 and 25: ○, σ_{43}; ◇, σ_{54}; △, σ_{53}; □, σ_{52}.

of scans like Fig. 2. From such plots and ratios of cross sections for σ_{54} of Ar^{5+} and σ_{21} of O^{2+} (Ref. 34), the error in N_i was estimated (less than 5%) and a correction was made.

A possible source of error in measured results is the presence of excited-state ions in the incident beam. Müller, Klinger, and Salzborn[35] maintain that there are no metastables in the beam of ions from their ion source, but that a metastable component is formed in charge transfer. By using a beam of ions formed by charge transfer as the incident beam in a second collision experiment, they observe significant enhancement of charge transfer and ionization for Ar ions in Ar. Dmitriev *et al.*[27] have also directly observed such enhancement due to metastables in the incident ion beam. They observe that ion beams produced by foil or gas stripping give higher apparent cross sections for ionization and slightly higher for charge transfer than beams produced directly in a PIG ion source. We have not yet made direct tests for the presence of metastable ions in the beam. However, indirect evidence, relying on the assertion that cross sections for charge exchange out of metastable ion states should be larger than from ground states, suggests no significant metastable contamination of present data. First, present data are lower than those of Klinger *et al.* which are asserted to be free of metastables. Second, as the incident ion beam charge state is changed, one would expect the fraction of metastables in the beam would change since Li-like ions should not be contaminated by metastables, whereas He-like or Be-like ions are likely to be. In the present case for N^{3+}, N^{4+}, and N^{5+} incident ions, the largest charge-transfer cross section is σ_{43}, which should be the least likely to be enhanced by excited states in the incident beam.

ACKNOWLEDGMENTS

The authors express gratitude to a number of people who have assisted with apparatus or taken an unusual interest in results. In particular, J. W. Hale, J. A. Ray, and I. A. Sellin have assisted in some way with apparatus; and C. F. Barnett and R. E. Olson have been helpful in frequent discussions of the results.

---

*Work supported, in part, by the U. S. Energy Research and Development Administration under contract with Union Carbide Corporation.

[1]G. Steigman, Astrophys. J. 199, 642 (1976).
[2]J. T. Hogan and H. C. Howe, J. Nucl. Mater. (to be published).
[3]W. H. Louisell, M. O. Scully, and W. B. McKnight, Phys. Rev. A 11, 989 (1975).
[4]A. V. Vinogradov and I. I. Sobel'man, Zh. Eksp. Theor. Fiz. 63, 2113 (1972) [Sov. Phys.–JETP 36, 1115 (1973)].
[5]M. L. Mallory and E. D. Hudson, IEEE Trans. Nucl. Sci. NS-22, 1669 (1975).
[6]M. L. Mallory and D. H. Crandall, IEEE Trans. Nucl. Sci. NS-23, 1069 (1976).
[7]G. A. Harrower, Rev. Sci. Instrum. 26, 850 (1955).
[8]Mullard, model No. B419BL.
[9]C. N. Burrous, A. J. Lieber, and V. T. Zaviantseff, Rev. Sci. Instrum. 38, 1477 (1967).
[10]A. Egidi, R. Marconero, G. Pizzella, and F. Sperli, Rev. Sci. Instrum. 40, 88 (1969).
[11]D. H. Crandall, J. A. Ray, and C. Cisneros, Rev. Sci. Instrum. 46, 562 (1975).
[12]P. Carr, Vacuum 14, 37 (1964).
[13]A. E. de Vries and P. K. Rol, Vacuum 15, 135 (1965).
[14]Charlotte E. Moore, *Atomic Energy Levels*, NBS Circ. No. 467 (U.S. GPO, Washington, D.C., 1949), Vol. 1.
[15]D. Rapp and W. E. Francis, J. Chem. Phys. 37, 2631 (1962).
[16]D. P. Hodgkinson and J. S. Briggs, J. Phys. B 9, 255 (1976).
[17]L. Landau, Sov. Phys. 2, 46 (1932).
[18]C. Zener, Proc. R. Soc. Lond. A 137, 696 (1932).
[19]L. P. Presnyakov and A. D. Ulantsev, Kvant. Electron 1, 2377 (1974) [Sov. J. Quant. Electron. 4, 1320 (1975)].
[20]A. Salop and R. E. Olson, Phys. Rev. A 13, 1312 (1976).
[21]D. H. Crandall, R. E. Olson, E. J. Shipsey, and J. C. Browne, Phys. Rev. Lett. 36, 858 (1976).
[22]E. J. Shipsey, J. C. Browne, and R. E. Olson, Phys. Rev. A (to be published).
[23]R. E. Olson and A. Salop, Phys. Rev. A 14, 579 (1976).
[24]H. Klinger, A. Müller, and E. Salzborn, J. Phys. B 8, 230 (1975).
[25]E. Salzborn, IEEE Trans. Nucl. Sci. NS-23, 947 (1976).
[26]G. J. M. Winter, D. J. Bierman, and W. F. Van de Weg, Phys. Lett. 31A, 170 (1970).
[27]I. S. Dmitriev, V. S. Nikolaev, Yu. A. Tashaev, and Yu. Z. Teplova, Zh. Eksp. Theor. Fiz. 67, 2047 (1974) [Sov. Phys.–JETP 40, 1017 (1975)].
[28]H. D. Betz, Rev. Mod. Phys. 44, 465 (1972).
[29]J. E. Bayfield and G. A. Khayrallah, Phys. Rev. A 11, 920 (1975).
[30]N. Bohr, K. Dan. Vidensk. Selsk. Mat.-Phys. Medd. 28, No. 8 (1948).
[31]H. C. Brinkman and H. A. Kramers, Proc. Acad. Sci. Amsterdam 33, 973 (1930).
[32]I. P. Flaks and G. N. Ogurtsov, Zh. Tech. Fiz. 33, 748 (1963) [Sov. Phys.-Tech. Phys. 8, 560 (1963)].
[33]E. Salzborn (private communication).
[34]T. Jorgensen, Jr., C. E. Kuyatt, W. W. Lang, D. C. Lorents, C. A. Sautter, Phys. Rev. 140, A1481 (1965).
[35]A. Müller, H. Klinger, and E. Salzborn, J. Phys. B 9, 291 (1976).